

Divergent Approach for *Tris*-Heteroleptic Cyclometalated Iridium Complexes Using Triisopropylsilylethynyl-Substituted Synthons

Robert M. Edkins, Yu-Ting Hsu, Mark A. Fox, Dmitry Yufit, Andrew Beeby,* and Ross J. Davidson*



Cite This: <https://doi.org/10.1021/acs.organomet.2c00292>



Read Online

ACCESS |



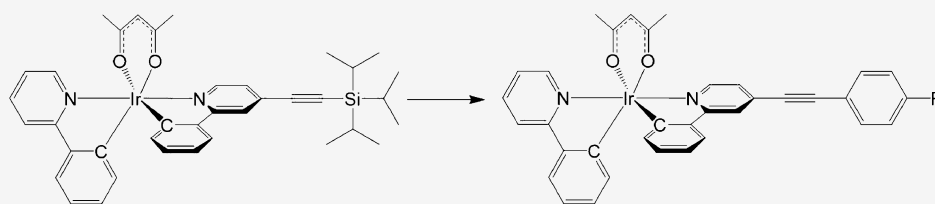
Metrics & More



Article Recommendations



Supporting Information



ABSTRACT: *Bis*-heteroleptic cyclometalated iridium complexes of the form $\text{Ir}(\text{L}^{\text{a}})_2(\text{acac})$, where L^{a} is a substituted 2-phenylpyridine derivative and acac is an acetylacetonato ligand, are a useful class of luminescent organometallic complexes for a range of applications. Related *tris*-heteroleptic complexes of the form $\text{Ir}(\text{L}^{\text{a}})(\text{L}^{\text{b}})(\text{acac})$ offer the potential advantage of greater functionality through the use of two different cyclometalated ligands but are, in general, more difficult to obtain. We report the synthesis of divergent *bis*- and *tris*-heteroleptic triisopropylsilylethynyl-substituted intermediate complexes that can be diversified using a “chemistry-on-the-complex” approach. We demonstrate the methodology through one-pot deprotection and Sonogashira cross-coupling of the intermediate complexes with *para*-R-aryliodides ($\text{R} = \text{H}$, SMe, and CN). The photophysical and electrochemical behaviors of the resultant *bis*- and *tris*-heteroleptic complexes are compared, and it is shown that the *tris*-heteroleptic complexes exhibit subtly different emission and redox properties to the *bis*-heteroleptic complexes, such as further red-shifted emission maxima and lower extinction coefficients, which can be attributed to the reduced symmetry. It is demonstrated, supported by DFT and time-dependent DFT calculations, that the charge-transfer character of the emission can be altered via variation of the terminal substituent; the introduction of an electron-withdrawing cyano group in the terminal position leads to a significant red shift, while the introduction of an SMe group can substantially increase the emission quantum yield. Most notably, this convenient synthetic approach reduces the need to perform the often challenging isolation of *tris*-heteroleptic complexes to a single divergent intermediate, which will simplify access to families of complexes of the form $\text{Ir}(\text{L}^{\text{a}})(\text{L}^{\text{b}})(\text{acac})$.

Iridium complexes containing a *bis*-heteroleptic arrangement $\text{Ir}(\text{N}^{\wedge}\text{C})_2(\text{A})$ (where $\text{N}^{\wedge}\text{C}$ is a 2-phenylpyridine-based ligand and $\text{A} =$ bidentate ancillary ligand) were first synthesized by Lamansky¹ in 2001 and have since become extensively used for applications such as organic light-emitting diodes (OLEDs),² biological imaging,³ and, more recently, photocatalysts.⁴ Their ubiquitous use can be attributed to their predictable structure–property relationships and controllable electronic structure, that is, the LUMO is predominantly localized to the pyridyl group, while the HOMO is localized to the iridium and phenyl groups, and, as such, any modifications at these positions can tune the emission color.^{5–9} Additionally, the emission lifetimes are typically in the microsecond range, with photoluminescent-quantum yields (PLQYs, Φ), in general, higher than those of other similar organometallic systems.

Despite *bis*-heteroleptic iridium complexes being well-established, there remain relatively few examples of *tris*-heteroleptic iridium complexes.¹⁰ It was not until we developed the approach of reacting two different 2-phenylpyridine-based ligands (L^{a} and L^{b}) with $\text{IrCl}_3 \cdot 3\text{H}_2\text{O}$ to form a mixture of iridium chloro-bridged dimers followed by reaction

with acetylacetonate to give a statistical mixture of $\text{Ir}(\text{L}^{\text{a}})_2(\text{acac})$, $\text{Ir}(\text{L}^{\text{a}})(\text{L}^{\text{b}})(\text{acac})$, and $\text{Ir}(\text{L}^{\text{b}})_2(\text{acac})$ species that $\text{Ir}(\text{L}^{\text{a}})(\text{L}^{\text{b}})(\text{acac})$ complexes could be separated by chromatography.^{10–12}

Following this, new approaches have been developed that initially use the degradation of a *tris*-cyclometalated to a mixed ligand iridium-chloro dimer, which was coordinated to an ancillary ligand to form a *tris*-heteroleptic complex.^{13–15} Adamovich et al. recently reported an approach that used an aryl-*N*-heterocyclic carbene ligand to form an intermediate iridium complex that favored the formation of mixed ligand chloro dimers, avoiding statistical distributions of products.¹⁶

Tris-heteroleptic complexes have the benefit of combining properties originating from each individual ligand–metal combination into a single complex that can be additive,

Received: June 13, 2022

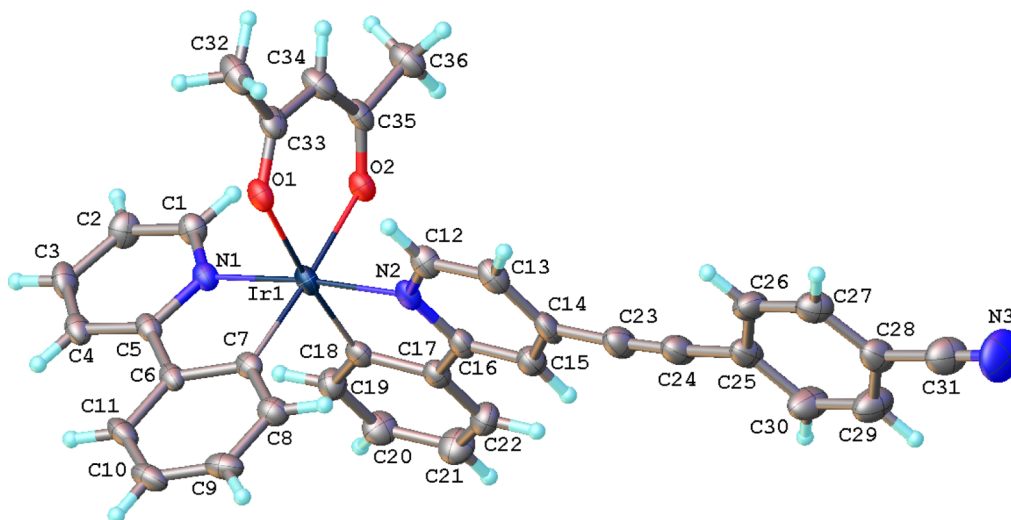


Figure 2. Molecular structure of 6. Thermal ellipsoids displayed at 50% probability.

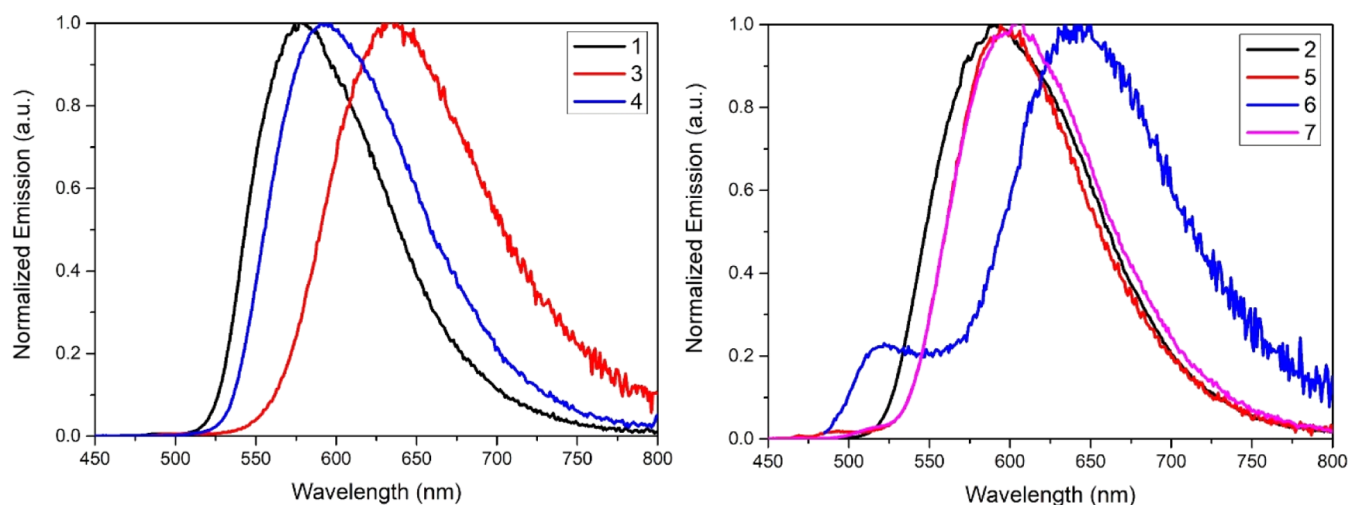


Figure 3. Steady-state emission spectra of *bis*-heteroleptic (left) and *tris*-heteroleptic (right) complexes 1–7 recorded in DCM.

Structural Analysis. The molecular structure determined by X-ray diffraction on a crystal of the *tris*-heteroleptic complex 6 is shown in Figure 2 (CCDC 2169136). Three virtually planar bidentate ligands comprise a typical octahedral coordination of the central iridium atom. The terminal 4-cyanophenylene group is also almost co-planar to the pyridine ring, connected to it via an alkyne; the corresponding dihedral angle is $6.2(1)^\circ$. The complexes within the crystal structure are linked together by a variety of weak intermolecular interactions such as $\text{CH}\cdots\text{N}$, $\text{CH}\cdots\pi$, and $\pi\cdots\pi$. The complexes form elliptical channels along the *a*-axis filled with disordered solvent molecules. The narrowest cross section of the channel is approximately 4 Å.

Electrochemistry. Cyclic voltammograms for complexes 2, 3, and 5–7 were recorded in 0.1 M TBAPF₆ in acetonitrile (MeCN), while the cyclic voltammogram for complex 4 was recorded in 0.1 M TBAPF₆ in dichloromethane (DCM) owing to its lower solubility (Figures S14–S19 and Table S4). Each of the complexes was internally referenced against ferrocene [i.e., $E_{1/2}(\text{Fc}/\text{Fc}^+) = 0.00$ V] and displayed a single oxidation event attributed to the characteristic Ir(III)/Ir(IV) couple. The nitrile complexes (3 and 6) showed a modest increase in oxidation potential (0.04 and 0.03 V, respectively) relative to

the other complexes in either the *bis*- or the *tris*-heteroleptic series. These increases suggest that the nitrile groups are sufficiently electron-withdrawing to impact the HOMO energy, which is typically located at the iridium and cyclometalated phenylene moiety. The potential differences in the nitrile complexes 3 and 6 with respect to other complexes are unexpected as the distance between the nitrile group and the iridium atom is over 11 Å in the structure of 6 (Figure 2).

In addition to the oxidation event, complexes 2, 3, and 5–7 displayed a reduction event attributed to the reduction of the ligand. For the *tris* complexes (5–7), this is most likely to be on the modified ppy ligand given the similar values found with the corresponding *bis*-heteroleptic analogues. Complexes 3 and 6 showed a 0.2 V cathodic shift relative to the other complexes due to the electron-withdrawing nature of the nitrile groups.

Photophysics. The electronic absorption spectra of the complexes were recorded in DCM (Figures S20, S21). Based on literature comparisons, each of the complexes displayed a ³MLCT [metal to ligand charge transfer (MLCT)] band at $\lambda = 450\text{--}600$ nm, a ¹MLCT band at $\lambda = 400\text{--}350$ nm, and a $\pi \rightarrow \pi^*$ transition at $\lambda < 350$ nm. The MLCT region is broad with a low extinction coefficient (ϵ), making observable differences between complexes difficult. However, in the $\pi \rightarrow \pi^*$ region,

Table 1. Photophysical Data for Complexes 1–7 Recorded in DCM^a

complex	λ_{emis}	PLQY (Φ)	lifetime (τ , μs)	$k_r \times 10^5 \text{ s}^{-1}$	$k_{\text{nr}} \times 10^5 \text{ s}^{-1}$	pure radiative lifetime (τ_0 , μs)
$\text{Ir}(\text{ppy})_2(\text{acac})^1$	520	0.71	1.90	2.55	3.73	1.52
$\text{Ir}(\text{ppy}\equiv\text{C}_6\text{H}_5)_2(\text{acac})^{2,4,b}$	570	0.28	0.93	3.01	7.74	3.32
1	580	0.65	1.20	5.42	2.92	1.84
2	588	0.69	1.40	4.93	2.21	2.03
3	639	0.15	0.22	6.64	38.8	1.51
4	600	1.00	0.91	11.0	0	0.91
5	603	0.52	0.95	5.47	5.05	1.83
6	646	0.086	0.16	5.38	57.1	1.86
7	608	0.585	1.10	5.32	3.77	1.88

^aThe radiative k_r and non-radiative k_{nr} values were calculated according to the equations: $k_r = \Phi/\tau$ and $k_{\text{nr}} = (1 - \Phi)/\tau$, from the quantum yields Φ and the lifetime τ values. ^bRecorded in toluene.

the *bis*-heteroleptic complexes (**1**, **3**, and **4**) have ca. double the ϵ of the *tris*-heteroleptic complexes (**2** and **5–7**), which can be attributed to the increased degeneracy of the *bis*-heteroleptic complexes owing to the increased symmetry.

The steady-state emission spectra were recorded in degassed solutions of DCM (see Figure 3, data summarized in Table 1). Each of the complexes (**1**, **2**, **4**, **5**, and **7**) displayed a broad emission at $\lambda = 500\text{--}750$ nm. Complexes **3** and **6** showed a broad emission at $\lambda = 550\text{--}800$ nm, significantly red-shifted compared to the previous complexes, due to the strong electron-withdrawing nature of the nitrile groups and the LUMO being localized to the 4-(phenylethynyl)pyridine component of the complex.

The *tris*-heteroleptic complexes revealed subtle red shifts in emission relative to their *bis* analogues in solutions; for example, there is a shift from $\lambda_{\text{em}} = 600$ nm to $\lambda_{\text{em}} = 608$ nm ($\Delta\nu = 219 \text{ cm}^{-1}$) when comparing the emission of complexes **4** and **7**. The red shift is attributed to the increased dipole moment associated with the asymmetric structure of the *tris*-heteroleptic complex through lifting of the degeneracy of the two cyclometalated ligands and would be consistent with the ³CT [charge transfer (CT)] character of the emission with the relatively short pure-radiative lifetimes of $\tau_0 = 0.91$ (**4**)– $2.03 \mu\text{s}$ (**2**). As a final means of testing the emission character, the emissions of the complexes were also recorded in cyclohexane, toluene, and acetonitrile solutions. All the complexes displayed a significant red shift in emission as the solvent polarity increased, confirming the emission to be ³CT in nature and, given the nature of the complexes, it is specifically a ³MLCT emission.

When complexes **3** and **6** were irradiated in DCM over a 60 min period, an additional emissive species was formed with an emission maximum (λ_{max}) of 500 nm (Figures S22 and S23). Although the specific nature of this emissive species could not be determined, it is attributed to a product of photodegradation of the initial complexes. This behavior was not observed for other complexes; as such, it must be formed either directly because of the nitrile group or because of its resulting electron deficiency. This photodegradation species appears to form more rapidly for complex **6** than for complex **3**.

A wide range of PLQYs were observed for complexes **1–7**, with the nitrile complexes **3** ($\Phi = 0.15$) and **6** ($\Phi = 0.086$) being low as a result of their high k_{nr} . In contrast, complex **4** exhibited a high PLQY, $\Phi = 1.00$. Jiang has suggested that the addition of thiomethyl groups to aza-BODIPYs enhances internal CT emissions,²³ but this warrants further investigation.

Computational Study. DFT calculations were performed on the optimized ground-state structures for complexes **1–7** with the model chemistry B3LYP/LANL2DZ/3-21G*. This model chemistry has been shown elsewhere to give a reasonable description of the electronic structure of organometallic iridium complexes.^{25,26} A comparison between the fully optimized geometry and the X-ray data for **6** revealed the Ir bond lengths to differ by less than 0.03 \AA (Table S5), which gives confidence in the suitability of this model chemistry for complexes **1–7**. The rotations of the aryl end groups attached to the ethynyl unit in **3–7** would be expected to be free in solution at ambient temperature; thus, different conformers of **3–7** present in solutions can influence the photophysical properties, including the absorption spectrum. The rotational barriers were estimated by constraining the aryl end groups to be perpendicular to the pyridyl ring attached to the ethynyl unit and found to be only ca. 4.2 kJ mol^{-1} in all cases. These constrained conformers are denoted with 90° here as in **3**(90°) and **6**(90°) for **3** and **6**(90°) for **6**.

Each of the complexes **1–7** showed a HOMO localized to the iridium and both phenylenes of the ppy ligand, as is typical for $\text{Ir}(\text{ppy})_2(\text{acac})$ -based complexes. The HOMO character is independent of the different substitutions made at the 4-position of the pyridyl ring as reflected in the similar observed oxidation potentials of 0.36 to 0.40 V for **1–7**. The HOMO characters remain unchanged with the constrained geometries (Figures 4 and S43–S48). The LUMOs of each of the complexes on the other hand are located on the pyridyl–

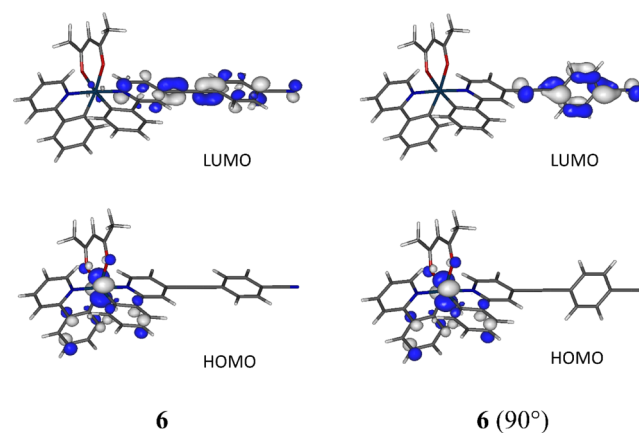


Figure 4. Frontier molecular orbitals for the fully optimized geometry **6** and the constrained geometry **6** (90°). Isocontours at $0.055 \text{ e bohr}^{-3/2}$.

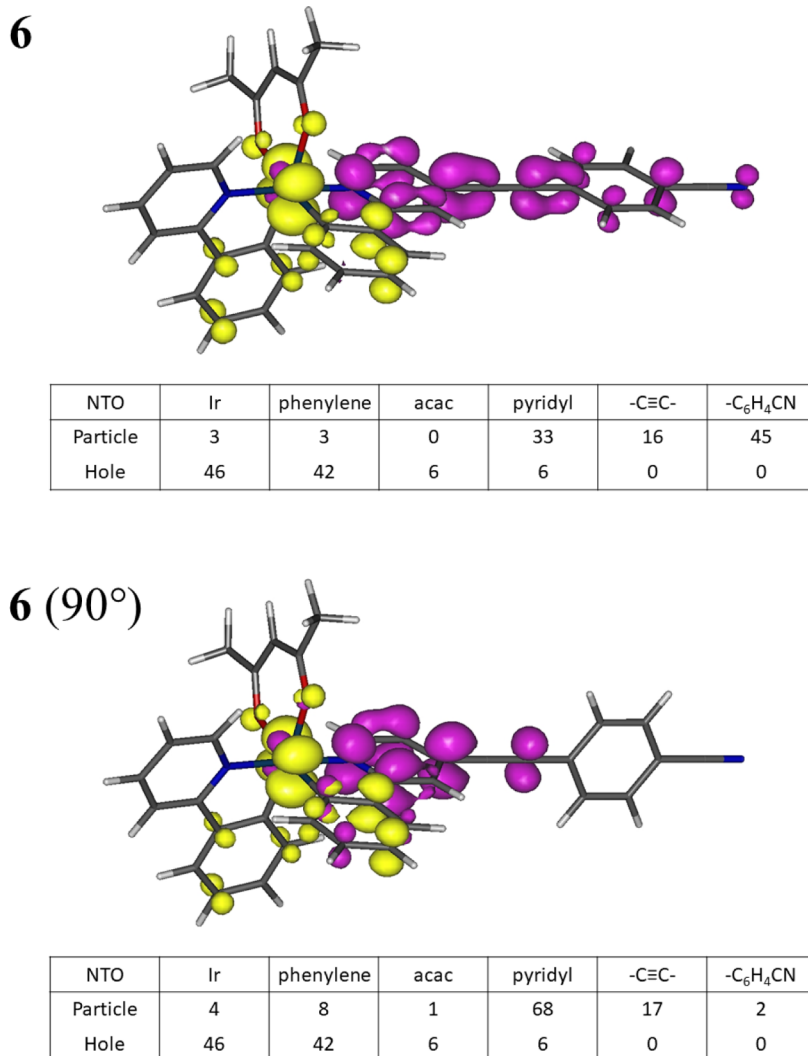


Figure 5. NTOs involved in the $S_0 \leftarrow T_1$ emissions for the fully optimized geometry **6** and the constrained geometry **6** (90°). Isocontours at $0.055 e \text{ bohr}^{-3/2}$.

ethynyl moiety and also on the aryl end groups for **3–7**. For the *bis*-heteroleptic complexes, the LUMO is in a degenerate state with equal contributions from both ligands, likely contributing to the higher PLQYs compared to their *tris*-heteroleptic analogues. The different LUMOs computed are in agreement with the varied reduction potentials observed where the less symmetrical *tris*-heteroleptic complexes **2**, **5**, **6**, and **7** have potentials at -2.33 , -2.23 , -1.97 , and -2.23 V, respectively. This potential trend is in agreement with the trend in their calculated LUMO energies (Table S7). The LUMOs differ between the fully optimized geometries **3–7** and the constrained analogues where the LUMOs are located at the pyridyl–ethynyl unit for **4**(90°), **5**(90°), and **7**(90°) and at the aryl end group for **3**(90°) and **6**(90°).

Time-dependent DFT calculations confirmed the expected $^3\text{MLCT}$ character of the $S_0 \leftarrow T_1$ transitions for the emissions of all complexes **1–7** based on mirroring the corresponding predicted $S_0 \rightarrow T_1$ transitions. By adjusting the calculated $S_0 \rightarrow T_1$ values with a simple scaling factor,²⁶ and taking into account both conformers in the case of **3–7**, the agreement with observed emission maxima for all complexes is excellent (Table S8). Natural transition orbitals involved in the NTOs involved in the $S_0 \leftarrow T_1$ transitions in all complexes **1–7** show

the expected hole orbital at the iridium–phenylene moiety where the phenylene is part of the ethynyl ppy ligand (Figures 5 and S49–S55). The particle orbital is located on the pyridyl–ethynyl moiety in these complexes with some contributions from the aryl end groups for **3–7**, accounting for the emission shift associated with the variation in substitution.

CONCLUSIONS

A versatile and divergent route to synthesizing *tris*-heteroleptic complexes has been demonstrated employing the TIPS-protected synthon complex **2**. This was shown to be readily modified via Sonogashira cross-coupling reactions to produce the *tris*-heteroleptic complexes **5–7** and, by utilizing the same approach, their *bis*-heteroleptic analogues could be synthesized from the previously reported TIPS-protected synthon complex **1**. The photophysical properties of both the *tris*- and *bis*-heteroleptic complexes were studied, revealing that each of the complexes had emissions that were ^3CT in character and significantly red-shifted relative to that of the parent complex $\text{Ir}(\text{ppy})_2(\text{acac})$. Additionally, varying the substituents of these complexes was shown to drastically impact the emission color, lifetime, and PLQY.

■ ASSOCIATED CONTENT

SI Supporting Information

The Supporting Information is available free of charge at <https://pubs.acs.org/doi/10.1021/acs.organomet.2c00292>.

NMR spectra, crystallographic data, photophysical data, and computational details (PDF)

Accession Codes

CCDC 2169136 contains the supplementary crystallographic data for this paper. These data can be obtained free of charge via www.ccdc.cam.ac.uk/data_request/cif, or by emailing data_request@ccdc.cam.ac.uk, or by contacting The Cambridge Crystallographic Data Centre, 12 Union Road, Cambridge CB2 1EZ, UK; fax: +44 1223 336033.

■ AUTHOR INFORMATION

Corresponding Authors

Andrew Beeby – Department of Chemistry, University of Durham, Durham DH1 3LE, U.K.; Email: andrew.beeby@durham.ac.uk

Ross J. Davidson – Department of Chemistry, University of Durham, Durham DH1 3LE, U.K.; orcid.org/0000-0003-3671-4788; Email: ross.davidson@durham.ac.uk

Authors

Robert M. Edkins – WestCHEM Department of Pure and Applied Chemistry, University of Strathclyde, Glasgow G1 1XL, U.K.; orcid.org/0000-0001-6117-5275

Yu-Ting Hsu – Department of Chemistry, University of Durham, Durham DH1 3LE, U.K.

Mark A. Fox – Department of Chemistry, University of Durham, Durham DH1 3LE, U.K.; orcid.org/0000-0002-0075-2769

Dmitry Yufit – Department of Chemistry, University of Durham, Durham DH1 3LE, U.K.

Complete contact information is available at: <https://pubs.acs.org/doi/10.1021/acs.organomet.2c00292>

Notes

The authors declare no competing financial interest.

■ ACKNOWLEDGMENTS

A.B. and R.J.D. gratefully acknowledge the EPSRC (EP/K007785/1; EP/K007548/1) for funding this work.

■ REFERENCES

- (1) Lamansky, S.; Djurovich, P.; Murphy, D.; Abdel-Razzaq, F.; Kwong, R.; Tsyba, I.; Bortz, M.; Mui, B.; Bau, R.; Thompson, M. E. Synthesis and Characterization of Phosphorescent Cyclometalated Iridium Complexes. *Inorg. Chem.* **2001**, *40*, 1704–1711.
- (2) Baldo, M. A.; Thompson, M. E.; Forrest, S. R. High-efficiency fluorescent organic light-emitting devices using a phosphorescent sensitizer. *Nature* **2000**, *403*, 750–753.
- (3) Lo, K. K.-W.; Li, S. P.-Y.; Zhang, K. Y. Development of luminescent iridium(III) polypyridine complexes as chemical and biological probes. *New J. Chem.* **2011**, *35*, 265–287.
- (4) Wang, P.; Guo, S.; Wang, H.-J.; Chen, K.-K.; Zhang, N.; Zhang, Z.-M.; Lu, T.-B. A broadband and strong visible-light-absorbing photosensitizer boosts hydrogen evolution. *Nat. Commun.* **2019**, *10*, 3155.
- (5) De Angelis, F.; Fantacci, S.; Evans, N.; Klein, C.; Zakeeruddin, S. M.; Moser, J.-E.; Kalyanasundaram, K.; Bolink, H. J.; Grätzel, M.; Nazeeruddin, M. K. Controlling Phosphorescence Color and Quantum Yields in Cationic Iridium Complexes: A Combined

Experimental and Theoretical Study. *Inorg. Chem.* **2007**, *46*, 5989–6001.

(6) Di Censo, D.; Fantacci, S.; De Angelis, F.; Klein, C.; Evans, N.; Kalyanasundaram, K.; Bolink, H. J.; Grätzel, M.; Nazeeruddin, M. K. Synthesis, Characterization, and DFT/TD-DFT Calculations of Highly Phosphorescent Blue Light-Emitting Anionic Iridium Complexes. *Inorg. Chem.* **2008**, *47*, 980–989.

(7) Takizawa, S.-y.; Nishida, J.-i.; Tsuzuki, T.; Tokito, S.; Yamashita, Y. Phosphorescent Iridium Complexes Based on 2-Phenylimidazo[1,2-a]pyridine Ligands: Tuning of Emission Color toward the Blue Region and Application to Polymer Light-Emitting Devices. *Inorg. Chem.* **2007**, *46*, 4308–4319.

(8) Avilov, I.; Minoofar, P.; Cornil, J.; De Cola, L. Influence of Substituents on the Energy and Nature of the Lowest Excited States of Heteroleptic Phosphorescent Ir(III) Complexes: A Joint Theoretical and Experimental Study. *J. Am. Chem. Soc.* **2007**, *129*, 8247–8258.

(9) Henwood, A. F.; Zysman-Colman, E. Lessons learned in tuning the optoelectronic properties of phosphorescent iridium(III) complexes. *Chem. Commun.* **2017**, *53*, 807–826.

(10) Tao, P.; Lü, X.; Zhou, G.; Wong, W.-Y. Asymmetric Tris-Heteroleptic Cyclometalated Phosphorescent Iridium(III) Complexes: An Emerging Class of Metallophosphors. *Acc. Mater. Res.* **2022**, DOI: [10.1021/accountsmr.2c00078](https://doi.org/10.1021/accountsmr.2c00078).

(11) Edkins, R. M.; Wriglesworth, A.; Fucke, K.; Bettington, S. L.; Beeby, A. The synthesis and photophysics of tris-heteroleptic cyclometalated iridium complexes. *Dalton Trans.* **2011**, *40*, 9672–9678.

(12) Liu, Z.; Xu, Y.; Yue, L.; Li, M.; Yang, X.; Sun, Y.; Yan, L.; Zhou, G. Iridium(III) complexes with the dithieno[3,2-b:2',3'-d]phosphole oxide group and their high optical power limiting performances. *Dalton Trans.* **2020**, *49*, 4967–4976.

(13) Baranoff, E.; Curchod, B. F. E.; Frey, J.; Scopelliti, R.; Kessler, F.; Tavernelli, I.; Rothlisberger, U.; Grätzel, M.; Nazeeruddin, M. K. Acid-Induced Degradation of Phosphorescent Dopants for OLEDs and Its Application to the Synthesis of Tris-heteroleptic Iridium(III) Bis-cyclometalated Complexes. *Inorg. Chem.* **2012**, *51*, 215–224.

(14) Tamura, Y.; Hisamatsu, Y.; Kumar, S.; Itoh, T.; Sato, K.; Kuroda, R.; Aoki, S. Efficient Synthesis of Tris-Heteroleptic Iridium(III) Complexes Based on the Zn²⁺-Promoted Degradation of Tris-Cyclometalated Iridium(III) Complexes and Their Photophysical Properties. *Inorg. Chem.* **2017**, *56*, 812–833.

(15) Tamura, Y.; Hisamatsu, Y.; Kazama, A.; Yoza, K.; Sato, K.; Kuroda, R.; Aoki, S. Stereospecific Synthesis of Tris-heteroleptic Tris-cyclometalated Iridium(III) Complexes via Different Heteroleptic Halogen-Bridged Iridium(III) Dimers and Their Photophysical Properties. *Inorg. Chem.* **2018**, *57*, 4571–4589.

(16) Adamovich, V.; Bajo, S.; Boudreault, P.-L. T.; Esteruelas, M. A.; López, A. M.; Martín, J.; Oliván, M.; Oñate, E.; Palacios, A. U.; Santorcuato, A.; Tsai, J.-Y.; Xia, C. Preparation of Tris-Heteroleptic Iridium(III) Complexes Containing a Cyclometalated Aryl-N-Heterocyclic Carbene Ligand. *Inorg. Chem.* **2018**, *57*, 10744–10760.

(17) Xu, X.; Guo, H.; Zhao, J.; Liu, B.; Yang, X.; Zhou, G.; Wu, Z. Asymmetric tris-Heteroleptic Iridium(III) Complexes Containing a 9-Phenyl-9-phosphafluorene Oxide Moiety with Enhanced Charge Carrier Injection/Transporting Properties for Highly Efficient Solution-Processed Organic Light-Emitting Diodes. *Chem. Mater.* **2016**, *28*, 8556–8569.

(18) Hisamatsu, Y.; Kumar, S.; Aoki, S. Design and Synthesis of Tris-Heteroleptic Cyclometalated Iridium(III) Complexes Consisting of Three Different Nonsymmetric Ligands Based on Ligand-Selective Electrophilic Reactions via Interligand HOMO Hopping Phenomena. *Inorg. Chem.* **2017**, *56*, 886–899.

(19) Zhang, Y.; Chen, X.; Song, D.; Zhong, D.; Yang, X.; Sun, Y.; Liu, B.; Zhou, G.; Wu, Z. Unsymmetric 2-phenylpyridine (ppy)-type cyclometalated Ir(III) complexes bearing both 5,9-dioxo-13b-boranaphtho[3,2,1-de]anthracene and phenylsulfonyl groups for tuning optoelectronic properties and electroluminescence abilities. *Inorg. Chem. Front.* **2020**, *7*, 1651–1666.

(20) Sun, Y.; Yang, X.; Liu, B.; Dang, J.; Li, Y.; Zhou, G.; Wu, Z.; Wong, W.-Y. Towards high performance solution-processed orange organic light-emitting devices: precisely-adjusting properties of Ir(III) complexes by reasonably engineering the asymmetric configuration with second functionalized cyclometalating ligands. *J. Mater. Chem. C* **2019**, *7*, 8836–8846.

(21) Boudreault, P.-L. T.; Esteruelas, M. A.; Mora, E.; Oñate, E.; Tsai, J.-Y. Suzuki–Miyaura Cross-Coupling Reactions for Increasing the Efficiency of *Tris*-Heteroleptic Iridium(III) Emitters. *Organometallics* **2019**, *38*, 2883–2887.

(22) Davidson, R.; Hsu, Y.-T.; Griffiths, G. C.; Li, C.; Yufit, D.; Pal, R.; Beeby, A. Highly Linearized Twisted Iridium(III) Complexes. *Inorg. Chem.* **2018**, *57*, 14450–14462.

(23) Jiang, X.-D.; Liu, X.; Fang, T.; Sun, C. Synthesis and application of methylthio-substituted BODIPYs/aza-BODIPYs. *Dyes Pigm.* **2017**, *146*, 438–444.

(24) Edkins, R. M.; Bettington, S. L.; Goeta, A. E.; Beeby, A. Two-photon spectroscopy of cyclometalated iridium complexes. *Dalton Trans.* **2011**, *40*, 12765–12770.

(25) Benjamin, H.; Fox, M. A.; Batsanov, A. S.; Al-Attar, H. A.; Li, C.; Ren, Z.; Monkman, A. P.; Bryce, M. R. Pyridylpyrazole NN ligands combined with sulfonyl-functionalised cyclometalating ligands for blue-emitting iridium(III) complexes and solution-processable PhOLEDs. *Dalton Trans.* **2017**, *46*, 10996–11007.

(26) Benjamin, H.; Zheng, Y.; Batsanov, A. S.; Fox, M. A.; Al-Attar, H. A.; Monkman, A. P.; Bryce, M. R. Sulfonyl-Substituted Heteroleptic Cyclometalated Iridium(III) Complexes as Blue Emitters for Solution-Processable Phosphorescent Organic Light-Emitting Diodes. *Inorg. Chem.* **2016**, *55*, 8612–8627.

Recommended by ACS

Cationic Iridium Complexes with 5-Phenyl-1H-1,2,4-triazole Type Cyclometalating Ligands: Toward Blue-Shifted Emission

Xiaoxiang Wang, Lian Duan, *et al.*

AUGUST 29, 2019
INORGANIC CHEMISTRY

READ 

Roles of Ancillary Chelates and Overall Charges of Bis-tridentate Ir(III) Phosphors for OLED Applications

Ling-Yang Hsu, Yun Chi, *et al.*

DECEMBER 11, 2019
ACS APPLIED MATERIALS & INTERFACES

READ 

Highly Luminescent Dinuclear Iridium(III) Complexes Containing Phenanthroline-Based Neutral Ligands as Chemosensors for Cu²⁺ Ion

Ze-Rong Ge, Tian-Yi Li, *et al.*

MARCH 11, 2022
ORGANOMETALLICS

READ 

Photo- and Electroluminescent Neutral Iridium(III) Complexes Bearing Imidoamidinate Ligands

Eugene A. Katlenok, Vadim Yu Kukushkin, *et al.*

JUNE 01, 2022
INORGANIC CHEMISTRY

READ 

Get More Suggestions >